Hearing the shape of a rod by the sound of its collision

Francesca M. F. Mascarenhas, C. M. Spillmann, John F. Lindner, and D. T. Jacobs
Physics Department, The College of Wooster, Wooster, Ohio 44691

(Received 25 July 1997; accepted 28 December 1997)

We collide rods of different lengths and infer the vibrational motion of the longer rod by a spectral analysis of the resulting sound. Collisions of rods of square and circular cross sections are audibly different. While longitudinal modes of vibration do not discriminate between different cross-sectional shapes, flexural modes do, and these enable us to hear the shapes of the rods. We use a microphone, an amplifier, and a spectrum analyzer to observe the longitudinal and flexural modes of the ringing rod. With an accessible mathematical model and a simple apparatus, we obtain good agreement between theory and experiment.

I. INTRODUCTION

The study of colliding rods has a long and rich history.[1–4] Recently, Auerbach[5] noted that colliding steel balls thud, while colliding steel rods ring. The collision of steel rods initiates vibrations in the steel that couple to the air to generate sound waves. We wondered if one could analyze the vibrations by merely listening to the sound of the collision. In fact, in the aftermath of a collision, these vibrations can be deduced from a spectral analysis of the ringing of one of the rods. This experiment uses simple equipment found in most undergraduate laboratories. Most interestingly, the sound of the collision reveals the shape of the cross section of the ringing rod.

II. THEORY

A. Vibrations confined to the longer rod

Auerbach[5] described how vibrations are confined to the longer of the two colliding rods. Figure 1 illustrates the mechanism of this confinement for longitudinal vibrations. A moving shorter rod collides with a stationary longer rod. Waves of expansion and compression bounce back and forth between the free ends of the rods at the speed of sound. At first, these waves pass through the collision interface because it is compressed. However, when the waves become confined to the longer rod, the uncompressed interface reflects them, trapping the waves in the longer rod. The vibrating longer rod pulls away from the now quiescent shorter rod. It is these vibrations, the ringing of the longer rod, that generate the sound we hear.

Note that the longer rod does not recoil with a single velocity. Only its center of mass moves uniformly, its velocity resulting from the conservation of momentum. In this inelastic collision, a fraction of the original kinetic energy is transformed into elastic energy, and ultimately dissipated as heat and sound.

B. Longitudinal wave equation

Upon colliding, longitudinal waves of compression and tension propagate in the longer rod. There are several differ-

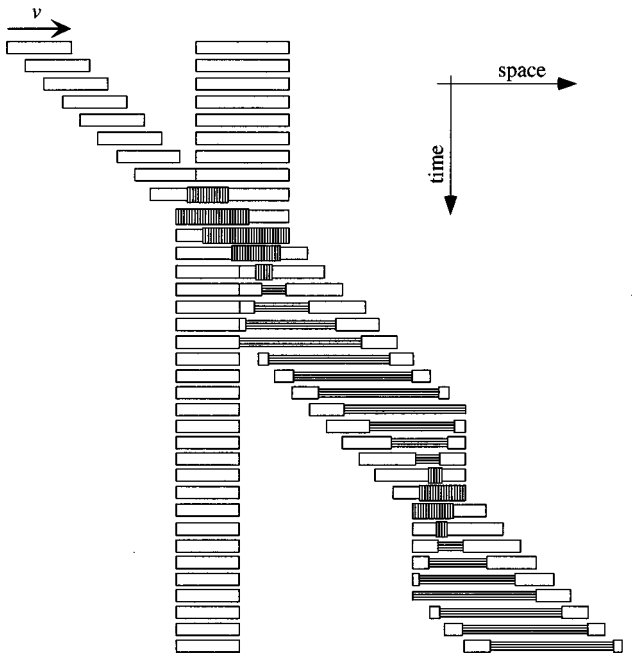

Fig. 1. Sequence from a computer simulation of the longitudinal vibrations resulting from the collision of a longer and a shorter rod. The longer rod is initially at rest and the shorter rod is initially moving left to right. The collision brings the shorter rod to a complete stop. The longer rod recoils as a longitudinal wave reflects back and forth across its length. Vertical hatching denotes compression and horizontal hatching denotes tension.

ent ways to analyze such waves. We will apply Newton's second law of motion and Hooke's law of elasticity to an infinitesimal element of the rod.[6] We will assume that the rod is long and thin.

Consider Fig. 2. An element of the rod lying between x and $x+dx$ is stretched so that its left edge displaces a distance ξ and its right edge displaces a distance $\xi+d\xi$. The *strain* is the relative change in length $\partial\xi/\partial x$, and the *stress* is the force per unit cross-sectional area F/A. According to Hooke's law, stress is proportional to strain, so

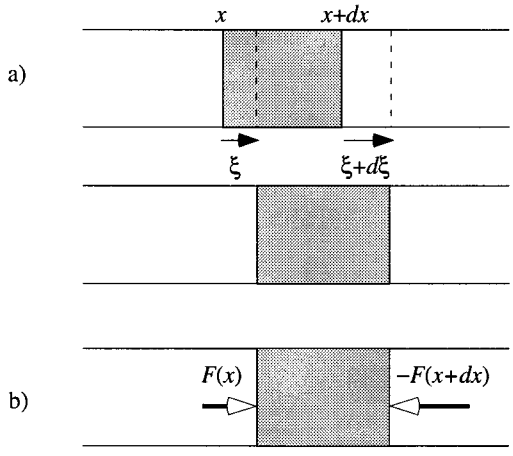

Fig. 2. Longitudinal stress and strain: (a) the strain in an infinitesimal stretched element of the rod, and (b) the stress. The force $-F(x+dx)$ on the right side of the element is the reaction to the force $+F(x+dx)$ on the rest of the rod to the right.

$$\frac{F}{A}=-E\,\frac{\partial\xi}{\partial x}, \tag{1}$$

where the proportionality constant E is Young's elastic modulus, and the negative sign ensures that, during compression, positive stress results in negative strain. The net force on the element is

$$dF=F(x)-F(x+dx)=-\frac{\partial F}{\partial x}\,dx. \tag{2}$$

According to Newton's second law, force equals mass times acceleration,

$$dF=dm\,\frac{\partial^2\xi}{\partial t^2}, \tag{3}$$

or, by combining Eq. (1) and Eq. (2),

$$AE\,\frac{\partial^2\xi}{\partial x^2}\,dx=\rho A dx\,\frac{\partial^2\xi}{\partial t^2}, \tag{4}$$

where ρ is the mass density of the rod, and hence

$$\frac{\partial^2\xi}{\partial x^2}=\frac{1}{c_L^2}\,\frac{\partial^2\xi}{\partial t^2}, \tag{5}$$

where $c_L=\sqrt{E/\rho}$. This second-order partial differential equation is the classical wave equation.

C. Longitudinal modes

We seek normal modes of longitudinal vibration by assuming

$$\xi(x,t)=(\alpha\,\cos\,kx+\beta\,\sin kx)\cos(\omega t+\varphi), \tag{6}$$

where the two constants α and β are determined by boundary conditions. By direct substitution, we find that this is a solution of Eq. (5) provided $\omega=kc_L$. The direct proportionality between the temporal and spatial frequencies indicates that the longitudinal waves are dispersionless. The group speed and phase speed of the longitudinal waves are both $\omega/k=c_L$.

In our experiment, after the rods separate, the ends of the rods are free. Hence, the stress must vanish at each end, $0=F=-AE\partial\xi/\partial x$, and the boundary conditions on the normal modes at $x=0$ and $x=L$ are

$$\frac{\partial\xi}{\partial x}=0. \tag{7}$$

The first of these requires $\alpha=\beta$. The second then requires $\sin kL=0$. Thus the spatial frequencies of the normal modes satisfy $k_nL=n\pi$ and the temporal frequencies are $2\pi f_n=\omega_n=k_nc_L$ or

$$f_n=n\,\frac{c_L}{2L}, \tag{8}$$

where $n=1,2,3,\ldots$.

D. Flexural wave equation

When a rod collides or is struck at one end, it is prone to vibrate transversely as well as longitudinally; in fact, the internal coupling between strains makes propagation of just one type of motion difficult to achieve. Even a slight eccentricity in the collision results in significant flexural vibra-

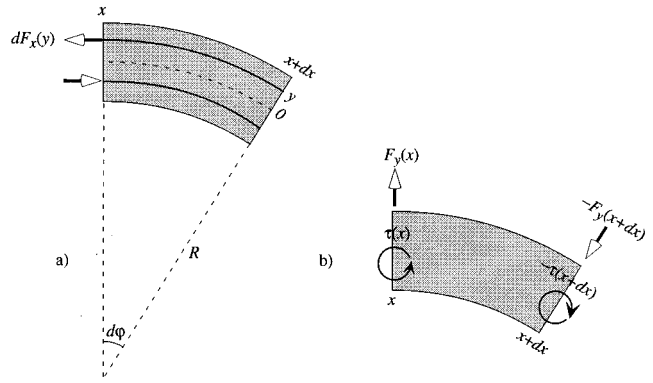

Fig. 3. Flexural stress and strain: (a) the strain in an infinitesimal bent element of the rod, and (b) the stress. The force $-F_y(x+dx)$ and torque $-\tau(x+dx)$ on the right side of the element is the reaction to the force $+F_y(x+dx)$ and torque $+\tau(x+dx)$ on the rest of the rod to the right.

tions. Moreover, flexural vibrations couple more efficiently to sound waves than longitudinal vibrations (because during flexural vibrations a larger surface area of the rod moves perpendicular to itself). Although there are several different ways to analyze such flexural waves,[7] we will again apply Newton's second law of motion and Hooke's law of elasticity to an infinitesimal element of the rod. We will assume that the rod is long and thin (so that the flexural wavelengths are small compared to the rod's diameter) and that the angles and displacements of the bends are small.

Consider Fig. 3. The outer part of the bent rod is stretched while the inner part is compressed. Assume that the point (x,y) displaces through (ξ,η). The longitudinal strain in an infinitesimal element a distance y from the neutral center line is $\partial\xi/\partial x$, and the longitudinal stress is dF_x/dA. According to Hooke's law,

$$\frac{dF_x}{dA}=-E\,\frac{\partial\xi}{\partial x}, \tag{9}$$

where the proportionality constant E is again Young's elastic modulus. dF_x is negative for outer filaments under tension and positive for inner filaments under compression. The strain can be expressed in terms of the radius of curvature R of the bend,

$$\frac{\partial\xi}{\partial x}=\frac{(R+y)d\varphi-Rd\varphi}{Rd\varphi}=\frac{y}{R}. \tag{10}$$

Although the total longitudinal force integrated across the cross section vanishes (tension above canceling compression below), there is a nonvanishing moment of force or torque about the neutral axis, $\tau=\int d\tau=\int y dF_x$. Invoking both Eq. (9) and Eq. (10), we may write

$$\tau=-\frac{EAR_G^2}{R}, \tag{11}$$

where

$$R_G^2=\frac{1}{A}\int y^2 dA \tag{12}$$

defines the radius of gyration R_G of the cross section. For a circular rod of diameter D, $R_G=D/4$. For a square rod of side D, $R_G=D/\sqrt{12}$.

If the angles of the rod are small, so that $\partial\eta/\partial x\ll 1$, we may approximate[8] the curvature of the bend as

$$\frac{1}{R}\approx\frac{\partial^2\eta}{\partial x^2}, \tag{13}$$

so that the expression for torque becomes

$$\tau=-EAR_G^2\,\frac{\partial^2\eta}{\partial x^2}. \tag{14}$$

Because the bending moment or torque $\tau(x)$ varies along the rod, the shearing force $F_y(x)$ must also vary so as to prevent the bent rod from rotating. By computing the torques about the left end of the element, we require the balance

$$F_y(x+dx)dx=\tau(x)-\tau(x+dx) \tag{15}$$

or

$$F_y=-\frac{\partial\tau}{\partial x}=EAR_G^2\,\frac{\partial^3\eta}{\partial x^3}. \tag{16}$$

The net transverse force on the element is

$$dF_y=F_y(x)-F_y(x+dx)=-\frac{\partial F_y}{\partial x}\,dx. \tag{17}$$

According to Newton's second law,

$$dF_y=dm\,\frac{\partial^2\eta}{\partial t^2}, \tag{18}$$

or, by combining Eq. (16), Eq. (17), and Eq. (18),

$$-AER_G^2\,\frac{\partial^4\eta}{\partial x^4}\,dx=\rho A dx\,\frac{\partial^2\eta}{\partial t^2}, \tag{19}$$

where ρ is the mass density of the rod, and hence

$$\frac{\partial^4\eta}{\partial x^4}=-\frac{1}{R_G^2c_L^2}\,\frac{\partial^2\eta}{\partial t^2}, \tag{20}$$

where $c_L=\sqrt{E/\rho}$. This is a fourth-order partial differential equation.

E. Flexural modes

We seek normal modes of flexural vibration by assuming

$$\eta(x,t)=(\alpha\cosh kx+\beta\sinh kx+\gamma\cos kx+\delta\sin kx)\cos(\omega t+\varphi), \tag{21}$$

where the four constants α, β, γ, and δ are determined by boundary conditions. By direct substitution, we find that this is a solution of Eq. (20) provided $\omega=k^2c_LR_G$. The quadratic relation between the temporal and spatial frequencies indicates that the flexural waves are dispersive.

In our experiment, the ends of the rods are free. Hence, the torque and the shear must vanish at each end, $0=\tau=-AER_G^2\partial^2\eta/\partial x^2$ and $0=F_y=EAR_G^2\partial^3\eta/\partial x^3$, and the boundary conditions on the normal modes at $x=0$ and $x=L$ are

$$\frac{\partial^2\eta}{\partial x^2}=0,\quad\frac{\partial^3\eta}{\partial x^3}=0. \tag{22}$$

These conditions require first that $\alpha=\gamma$ and $\beta=\delta$, and then that

$$\alpha(\cosh kL-\cos kL)=\beta(\sin kL-\sinh kL),$$
$$\alpha(\sinh kL+\sin kL)=\beta(\cos kL-\cosh kL). \tag{23}$$

Taking the quotient of these two equations and employing several trigonometric and hyperbolic identities, we find that

$$\tan\left(\frac{kL}{2}\right)=\pm\tanh\left(\frac{kL}{2}\right). \tag{24}$$

We may solve this transcendental equation by plotting the left side versus the right side and recording the points of intersection. To a good approximation, we find

$$k_nL\approx\pm\frac{\pi}{2}(2n+1). \tag{25}$$

The temporal frequencies must therefore satisfy $2\pi f_n=\omega_n=k^2c_LR_G$ or

$$f_n\approx(2n+1)^2\frac{\pi c_LR_G}{8L^2}, \tag{26}$$

where $n=1,2,3,\ldots$.

Note that the flexural frequencies, given by Eq. (26), depend on the radius of gyration R_G (and hence the shape) of the cross section, while the longitudinal frequencies, given by Eq. (8), are independent of the cross section.

F. Corrections for thick rods

Our analysis is correct only for thin rods, or ''Euler–Bernoulli beams.'' For thick rods, or ''Timoshenko beams,'' effects such as rotary inertia and shear deformation must be considered. Both these effects will lower the frequencies of the flexural modes, especially the higher ones.[9]

Heuristically, the square of a vibrational frequency is the restoring force per unit displacement per unit inertia.[10] When a thick rod bends, its differential elements rotate through small angles. The corresponding rotational inertia depresses the vibrational frequencies. Also, as a thick rod bends, shear forces tend to deform it, skewing rectangular elements into parallelograms. The resulting mushy response reduces the restoring force and further depresses the vibrational frequencies.

III. EXPERIMENT

A. Apparatus and procedure

Initially, we set out to observe the collision between a shorter and a longer rod both visually and audibly. Without a high speed video camera, recording a collision and obtaining meaningful quantitative data is difficult. However, *listening* to the collision provided a rich sound which allowed even untrained ears to distinguish between square and circular cross-section rods. The nonharmonic frequencies present in the ringing of the longer rod (the shorter rod does not produce sound in the audible range) were found to be quite consistent with the flexural modes described above and to also include the longitudinal mode, which is responsible for the short rod transferring all of its momentum to the long rod as described by Auerbach[5] and demonstrated in our simulation (Fig. 1).

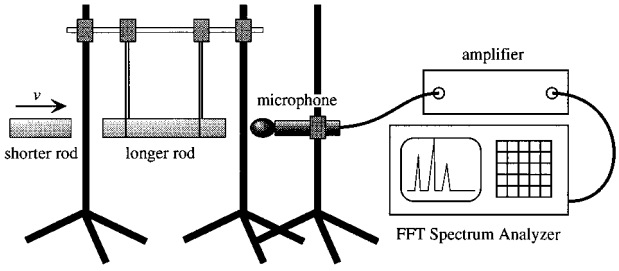

Fig. 4. Experimental apparatus. Fishing line suspends the longer rod horizontally. A microphone, an amplifier, and a spectrum analyzer record the sound of a longer rod after being struck horizontally by a shorter rod.

The rods we collided were machined from a single piece of cold-rolled stainless steel. We used two sets of longer (19.0 cm) and shorter (4.41 cm) rods to gather data; one set with square cross sections, the other with circular cross sections, and both of the same thickness (1.91 cm). Our apparatus is depicted in Fig. 4. The longer rod was suspended from a horizontal beam with fishing line, looping the fishing line around the ends of the rod, and then clamping the line to the beam above so that the long rod was suspended horizontally. Since we were interested in the frequencies present and not in the relative amplitudes, the support points were not varied. We clamped a microphone to a stand next to the end of the longer rod; however, our results were indifferent to either the placement of the microphone or acoustic reflections. We employed an inexpensive microphone to listen to the sound of the collision and a car audio amplifier (Radio Shack Optimus 100W) to amplify the signal before sending it to a FFT (fast Fourier transform) Spectrum Analyzer (Stanford Research System's SR760) where the data were recorded to disk and transferred to a computer for plotting and analysis.

Although we experimented with more elaborate techniques, we found it sufficient to collide the rods manually. We held the shorter rod in one hand, sharply knocked it against one end of the longer rod, and immediately retracted it. Such collisions easily generated reproducible sounds. While the longer rod rang for at least 1 min before the sound it generated decayed, we collected data about 1 s after the collision, while the principal acoustical peaks were still strong. While the relative intensities of the peaks might vary between trials, the locations of the peaks were very stable. The lowest frequencies were the most persistent and dominated the sound production after a few seconds.

B. Results and analysis

Typical audio frequency spectra for collisions between rods of square and circular cross section are shown in Fig. 5. The spectra are dominated by a small number of large peaks corresponding to the frequencies of the standing waves developed in Sec. II. The collision excites these standing waves which produce an audible sound corresponding to the first three flexural modes and the first longitudinal mode. Table I compares the locations of the experimental peaks to the lowest theoretical modal frequencies, using the speed of sound in steel[11] as $c_L=5100$ m/s. In agreement with the theory, the longitudinal peaks occur at the same frequency for both square and circular rods, but the flexural peaks of the square rods are shifted about $\sqrt{4/3}\approx1.15$ times higher than the flex-

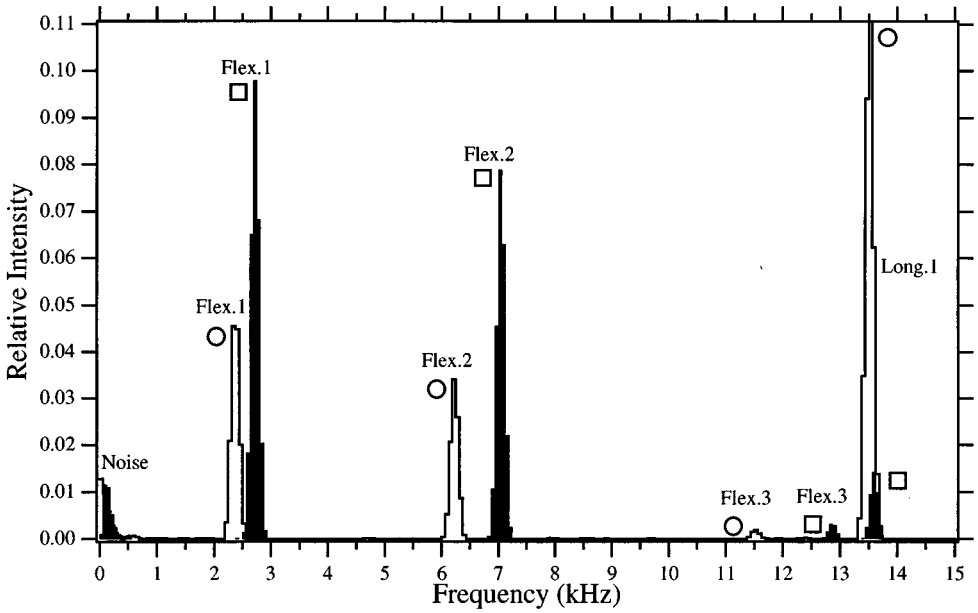

Fig. 5. Acoustical spectra of the sounds of the collisions of longer and shorter rods of square (black) and circular (white) cross sections. The shapes of the rods separate the first three flexural peaks, but the longitudinal peaks coincide. For theoretical values, consult Table I.

ural peaks for the circular rods. This factor is the ratio of the radii of gyration of the square and circular rods, according to Eq. (26). Roughly speaking, the square cross section places more steel farther from the neutral axis, compared to the circular cross sections, thereby increasing both the flexural restoring force and the flexural frequencies. However, contrary to the theory, the higher flexural frequencies are about 10% lower than predicted. This is because our longer rods, with a length to thickness ratio of only about 6.4, were not very thin, and hence only approximated the Euler–Bernoulli beams in the simple theory presented above.

The distinct shift in frequency between square and circular cross-section rods is distinctly audible, measurable, and consistent with a simple theory accessible to undergraduates. The quantitative measurement of the shift described above uses a commercial FFT spectrum analyzer, but the first flexural frequency can easily be measured using data acquisition systems and software in common use in general physics labs. Using Pasco Scientific's interface hardware (CI 6560) along with Pasco's Science Workshop software, a FFT of the amplified audio gives sharp peaks for the first flexural mode with values consistent with those reported here. Thus quantitative measurements can be made relatively easily and compared to theory. Hearing rods ring gives great insight into the audible frequencies of many common devices from chimes to xylophones.

Table I. Theoretical and experimental frequencies of vibration, for rods of square and circular cross section, assuming the speed of sound in steel $c_L = 5100$ m/s.

	Longitudinal	Flexural		
	f_1 (kHz)	f_1 (kHz)	f_2 (kHz)	f_3 (kHz)
Square				
theory	13.5	2.78	7.73	15.1
experiment (± 0.25 kHz)	13.6	2.63	7.00	12.9
Circular				
theory	13.5	2.41	6.69	13.1
experiment (± 0.25 kHz)	13.5	2.38	6.25	11.5

IV. CONCLUSION

By a spectral analysis of the ringing sound following the collision of steel rods, we can infer the vibrational motion of the rods. Rods of square and circular cross section generate sound that is different to the ear. With a microphone, an amplifier, and a spectrum analyzer, one can experimentally quantify this difference, and understand it theoretically, by the elementary analysis presented here. Our experimental resonant frequencies were in good agreement with our theory, and we anticipate even better agreement with thin rods. It is quite easy to hear the shape of a rod.

ACKNOWLEDGMENTS

We thank Jamie White for helpful discussions, the Wayne County Machine Shop for machining our steel rods, and the referees for helpful comments.

[1]Classic 19th century references include the following: B. Saint-Venant, ''The longitudinal impact of two bars'' (in French), Liouv. J. Math. **12**, 237–377 (1867); L. Boltzmann, ''Experiments on the impact of cylinders'' (in German), Wien. Ber. **84**, 1225–1229 (1881); H. Hertz, ''The contact of solid elastic bodies'' (in German), Crelles J. **92**, 156–172 (1882).
[2]J. W. S. Rayleigh, *The Theory of Sound* (Dover, New York, 1945), Vol. 1, Chaps. 7–8.
[3]J. F. Ball, in *Handbuch der Physik*, edited by S. Flügge (Springer, New York, 1973), Vol. VI a 11, pp. 313–331.
[4]W. G. B. Britton, J. J. Fendley, and M. E. Michael, ''Longitudinal impact of rods: A continuing experiment,'' Am. J. Phys. **46**, 1124–1130 (1978).
[5]D. Auerbach, ''Colliding rods: Dynamics and relevance to colliding balls,'' Am. J. Phys. **62**, 522–525 (1993).
[6]Our analysis is based on E. Kinsler, A. B. Coppens, A. R. Frey, and J. V.

Sanders, *Fundamentals of Acoustics* (Wiley, New York, 1982), 3rd ed., Chap. 3.
[7]G. Vandegrift, ''Transverse bending waves and the breaking broomstick demonstration,'' Am. J. Phys. **65**, 505–510 (1997).
[8]The general expression for curvature is derived in most introductory calculus texts, such as E. W. Swokowski, M. Olinick, D. Pence, and J. A. Cole, *Calculus* (PWS, Boston, 1994), 6th ed., Sec. 11.4.
[9]T. D. Rossing and N. H. Fletcher, *Principles of Vibration and Sound* (Springer-Verlag, New York, 1997), Sec. 2.17.
[10]For a harmonic oscillator, $\omega^2 = k/m = F/mx$. For more on the physical meaning of ω^2, consult F. S. Crawford, Jr., *Waves* (McGraw–Hill, New York, 1968), Sec. 1.2.
[11]*CRC Handbook of Chemistry and Physics*, edited by D. R. Lide and H. P. R. Frederikse (CRC, Boca Raton, FL, 1996), pp. 14–36.